ULTRA-HIGH TEMPERATURE CERAMICS FOR HYPERSONIC ENTRY OF SLENDER-SHAPED ADVANCED SPACE VEHICLES

M. Balat-Pichelin[(1)], E. Bêche[(1)], F. Monteverde[(2)], L. Scatteia[(3)], D. Alfano[(3)]

[(1)] *PROMES-CNRS, 7 rue du four solaire, 66120 Font-Romeu - Odeillo, France, Email: marianne.balat@promes.cnrs.fr*
[(2)] *ISTEC-CNR, 64 via Granarolo, 48018 Faenza, Italy, Email: frederic.monteverde@istec.cnr.it*
[(3)] *CIRA - Centro Italiano Ricerche Aerospaziali, 81043 Capua, Italy, Email: l.scatteia@cira.it*

ABSTRACT

The objective of this paper is to present and discuss the results of the catalytic properties of two Ultra High-Temperature Ceramics (UHTC) materials based upon the ZrB_2/SiC composition. Moreover, samples machined by diamond-loaded tools (DLT) and samples machined by electrical discharge machining (EDM) were tested to assess the effect of the surface finish (different surface roughness, partial oxidation during machining) upon those properties. The catalycity of these materials is then compared to the ones measured on different sintered zirconia, stabilized by yttria or calcia. Also, a comparison is done with the oxides obtained during air plasma and high temperature exposure on SiC, AlN and with quartz.
Micro-structural analyses by SEM and XPS have shown oxidation-induced surface modifications of ZrB_2/SiC materials with oxide layers composed of silica with trace amounts of boron oxide and zirconia if the maximum reached temperature is lower than about 1800 K and only zirconia for higher temperature values. The differences in the oxide layer composition may account for the different catalytic behavior. The higher recombination coefficients measured in the case of ZrB_2/HfB_2/SiC materials can be correlated with the presence of hafnia, probably characterized by higher catalytic activity compared to zirconia.

1. INTRODUCTION

Catalytic recombination of dissociated atmospheric oxygen molecules on the surface of thermal protection systems (TPS) located on nose and leading edges can be a significant additional heat source during the atmospheric re-entry of a space vehicle. Typically, TPS of re-entry vehicles are designed considering the constituent materials as fully catalytic, a strongly conservative assumption that can lead to an over-sizing of the total mass required for the TPS. However, mass, performance, and cost considerations in future re-usable re-entry vehicles require a more sensible design approach based upon a more realistic assumption of partial catalycity.
Ground test simulation under atmospheric re-entry conditions is therefore necessary to characterize and select base materials for TPS. Very high temperature and low pressure air plasma are reproduced within the MESOX facility – out of equilibrium plasma – with a degree of dissociation of oxygen reaching 70 % for an earth entry phase.
In this paper, experimental results are given on the catalytic properties of zirconium-based ceramics that represent a promising class of new TPS materials for the manufacturing of slender-shaped hot structures in hypersonic re-entry vehicles.
Two different zirconium-based compounds, produced by hot pressing and machined into their final shape by mean of electrical discharge machining or, alternatively, by diamond-tooling were tested in the temperature range 900-2500 K. Two kinds of zirconia different by their sintering additives were also tested in the same temperature range. The effects of the crystalline structure of zirconia materials and the one of surface machining for the zirconium-based ceramics are underlined and new experimental results on the recombination coefficient of atomic oxygen are obtained at high temperature on this class of new TPS.

Transition metal diborides such as ZrB_2 and HfB_2 are commonly referred to as Ultra High-Temperature Ceramics (UHTC) for their melting temperatures greater than 3300 K. Their physical characteristics enable applications at temperatures above 2000 K, a typical temperature limit of most structural ceramics. In particular, aerospace research in the past decades has been focused on UHTC as candidate materials to increase the heat tolerance resistance of structural TPS such as leading edges and nose-cones for sharp-shaped hypersonic re-entry vehicles [1-3]. The expected temperatures are above the operational single-use temperature limit of current TPS materials such as SiC-coated C/C composites. Progress has been made in the production of ZrB_2-based dense bodies with acceptable thermo-physical and mechanical properties and also in

their machining into complex-shaped components [3-5]. Among the open points of research on UHTC materials is the characterization of surface properties like catalycity in the high temperature range [6-8].
The objective of this paper is to present and discuss the results of catalytic properties of UHTC materials based upon the ZrB_2/SiC composition; more specifically, samples machined by diamond-loaded tools (DLT) and samples machined by electrical discharge machining (EDM) were tested to assess the effect of the surface finish (different surface roughness, partial oxidation during machining) upon those properties. The catalycity of these materials is then compared to the one measured on different sintered zirconia, stabilized by yttria or calcia. Also, a comparison is done with the oxides formed during the high temperature and air plasma exposure on SiC, AlN and with quartz.

2. MATERIALS AND EXPERIMENTAL

ZrB_2-based UHTC materials with different composition and surface finishing were used: ZrB_2/SiC (A) and ZrB_2/HfB_2/SiC (B). These materials were elaborated in Italy (CNR-ISTEC, Faenza) [3, 4]. They were obtained by hot pressing of the following two powder compositions (vol %):

- Material A: ZrB_2 + 15 SiC
- Material B: ZrB_2 + 15 SiC + 10 HfB_2

with 2 vol.% $MoSi_2$ as a sintering aid in both compositions. The two sintered materials were cut and shaped in billets of 25 mm diameter and 2 mm thickness for catalycity measurements using either diamond-loaded tools (DLT) or electrical discharge machining (EDM).
Two stabilized zirconia containing Y_2O_3 (YSZ) or CaO (CSZ) as sintering aids (3-5%) were used to measure the recombination coefficient. The choice of these zirconia samples to study the recombination of atomic oxygen was made according to the fact that we have previously shown that the crystal lattice is an important parameter to take into account for the catalycity; for example, β-cristobalite is more catalytic than quartz by nearly one order of magnitude [9]. So, we chose zirconia with different microstructures due to the presence of several impurities in low content to see if it is an influent parameter on catalycity as we have already shown on alumina samples [10]. Moreover, zirconia is a high stable refractory oxide that allows to perform measurement of the recombination coefficient until very high temperatures (2500 K) to eventually measure a change in the curve Log $\gamma = f(1/T)$. Zirconia is also part of the oxides formed during the oxidation of the UHTC like ZrB_2/SiC and ZrB_2/HfB_2/SiC.

The MESOX facility (Fig. 1) is described in details elsewhere [9], here only its main features are outlined. The ceramic sample is put in a plasma reactor consisting of a silica tube (quartz), 50 cm length and 5 cm diameter with CaF_2 viewports. The air plasma is generated by a 300 W microwave discharge surrounding the sample. A regulator, a gauge and a vacuum pump allow the precise control of the total pressure during experiments. The airflow is fixed at 4 l/h and is coming from to the top of the reactor and then pumped down. The sample is placed on a sample-holder at the centre of the plasma discharge. The reactor is positioned in such a way to let the sample be at 25 mm above the theoretical focus of the 6 kW solar furnace equipped with a variable opening shutter. The maximum incident concentrated solar flux can reach 5 $MW.m^{-2}$.

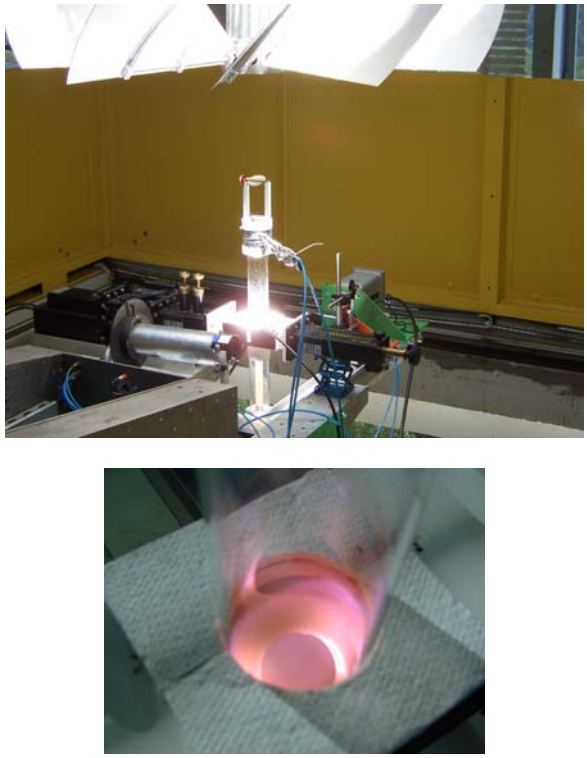

Fig. 1: MESOX facility at the focus of the 6 kW solar furnace (top) and image of the air plasma (down)

The spectroscopic bench used for Optical Emission Spectroscopy (OES) is composed of an optical sampling system including a lens and a mirror, and a monochromator (spectrometer Triax 550 Jobin-Yvon) equipped with an Optical Multichannel Analyzer (OMA). The microwave discharge is imaged by the silica lens (magnification 0.1) on the slit entrance of the monochromator. The 55 cm focal length monochromator working with a 1200 grooves/mm grating and a 100 μm width slit allows a spectral resolution of 0.2 nm. The dispersed light is analyzed by means of the CCD matrix (1024 x 128) of the OMA detector. Each of the 128 lines of the matrix gives

information on the relative atomic oxygen concentration at different distances from the surface of the sample with a spatial resolution around 270 µm. A spectral analysis over the 128 lines is performed very quickly after the solar radiation breaking. The total duration of a scan is 200 ms. Therefore all the spectral and spatial information are taken simultaneously allowing a good accuracy.

The recombination coefficient γ is defined as the ratio of the flux of recombined atoms to the total flux of atoms impinging the surface:

$$\gamma = O_{rec}/O_{tot} \quad (1)$$

In this section, the method used for the measurement of the recombination coefficient γ of atomic oxygen on surface is briefly presented as it is detailed in [9].
OES and actinometry techniques were used to follow the relative atomic oxygen concentration profile along the discharge. A low and known quantity of argon (5%) is introduced in the airflow and the evolution of the intensities ratio I_O/I_{Ar} of the 844.6 nm (O line) and 842.4 nm (Ar line) is measured along the discharge zone through the window (30 mm height and 9 mm width) performed in the waveguide. A cylindrical volume corresponding to the discharge zone is considered with every point represented by the coordinates (r, x). As the mean free path of oxygen atoms is 100 times less than the diameter of the reactor, the atom diffusion is given by the diffusion equation written in cylindrical coordinates that describes the variation of the oxygen concentration versus time for a fixed point (r, x) in the cylinder.
The experiments are performed in steady state conditions. The radial gradient in the reactor is negligible compared to the axial one, so the oxygen concentration is only function of x. Moreover, the stability of the I_O/I_{Ar} ratio in the reactor, measured without sample, allows neglecting the recombination in volume and on the reactor wall.
The intensities ratio profile leads to the determination of the recombination coefficient γ from the following equation:

$$\gamma = \left(\frac{\left.\frac{I_O}{I_{Ar}}\right|_{x=L}}{\left.\frac{I_O}{I_{Ar}}\right|_{x=0}} \cdot \frac{T_S}{T_L} - 1 \right) \frac{4.D_{O,air}}{V.L} \quad (2)$$

with $D_{O,air}$ the binary diffusion coefficient of O in air, V the mean square atomic oxygen velocity and L the thickness of the recombination boundary layer determined experimentally. Due to the temperature gradient between the sample (T_s) and the plasma bulk (T_L), the relative oxygen concentration ratio is related to the measured intensities ratio I_O/I_{Ar} respectively at the entrance of the reactor (x = L) and at the surface sample (x = 0). The partial pressure of the actinometer gas is assumed constant. The accuracy on γ has been estimated to be ± 30 %.
In the experimental conditions chosen for the measurement of γ, the density of oxygen atoms is around 9×10^{21} m^{-3} and the degree of dissociation is 70% [11].
A typical relative atomic oxygen profile above a zirconia sample at 2230 K is presented in Fig. 2. One can see that close to the surface, in the 3-4 mm, there is a decrease of the intensity ratio due to the recombination of oxygen atoms; then, far from the sample, this ratio is constant (here equal to almost 8) and not affected by the surface. This type of graphic is used for the determination of the measured intensities ratio I_O/I_{Ar} respectively at the entrance of the reactor (x = 16) and at the surface sample (x = 0) and for the calculation of the thickness of the recombination boundary layer L.

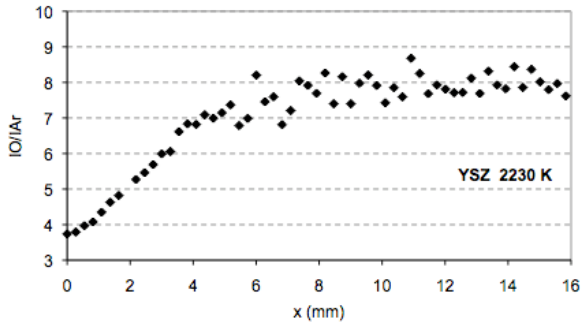

Fig. 2: Typical profile of the ratio of atomic oxygen and argon intensities versus the distance from the sample surface for a zirconia sample at 2230 K.

3. CATALYCITY OF ZrB_2/SiC-BASED UHTC MATERIALS

The catalycity data are hereby discussed by comparing the two materials A (ZrB_2/SiC) and B (ZrB_2/HfB_2/SiC) and, for EDM and DLT (different surface finish).
Figs. 3 and 4 reproduced the results obtained for the recombination coefficient on the four materials: A-EDM and A-DLT (Fig. 3), B-EDM and B-DLT (Fig. 4).
In the temperature range 900-2000 K, A-DLT (ZrB_2/SiC) shows higher catalytic activity than the A-EDM material. This behavior is due to the presence of a thin oxide layer formed during EDM, which is consistent with reports showing that amorphous and crystalline silicon oxides have low catalytic activity for oxygen recombination. As can be seen in Fig. 3, at about 1200 K, the γ curve of A-EDM exhibited a change in the slope: at temperatures lower than 1200 K, the recombination coefficient is almost constant

(around 8.10^{-3} close to the quartz one [9]). It is evident that the function ln γ = f(1/T) does not follow an Arrhenius type law that predicts a linear behavior in all the temperature range. This catalytic behavior of the A-EDM sample is confirmed the analogous experimental data obtained on sintered zirconia samples related to the monoclinic (M) to tetragonal (T) phase transformation of the zirconia present in the oxide layer (see after, section 4). It is important to point out that this double-slope trend does not occur in the A-DLT sample, thus suggesting that the surface finish and/or the surface micro-damage and oxidation occurring during EDM may play a significant role in defining the catalytic behavior of this UHTC composition. This is confirmed by the XPS analyses of the surfaces of the two samples A-EDM and A-DLT after γ measurement (Table 1).

On the contrary, a less evident difference is recorded between the γ values of B-DLT and B-EDM samples (Fig. 4). Both samples exhibit γ values ranging from 10^{-2} and 10^{-1} across the investigated temperature range and follow Arrhenius-like temperature dependence, just like the sample A-DLT.

The recombination coefficients γ have been calculated using the measured concentration profiles, obtained in steady-state conditions and are plotted on a logarithmic scale as a function of the reciprocal temperature for analysis by the Arrhenius equation:

$$\gamma = B \exp(-E_a/RT) \qquad (3)$$

where B is the pre-exponential coefficient, E_a is the activation energy of the oxygen recombination process, R the perfect gas law constant and T is the temperature. The Arrhenius fit gives the following expressions for the recombination coefficient γ and the respective activation energies E_a:

For ZrB_2/SiC EDM:

$\gamma \approx 8.10^{-3}$ up to 1200 K (before the M->T phase transformation)

$\gamma = 0.1426 \exp(-3285/T)$ from 1200 to 2000 K with $E_a \approx 27$ kJ mol^{-1}

For ZrB_2/SiC DLT:

$\gamma = 0.4722 \exp(-2951/T)$ up to 1840 K with $E_a \approx 24$ kJ mol^{-1}

For ZrB_2/HfB_2/SiC EDM:

$\gamma = 0.3463 \exp(-2288/T)$ up to 1820 K with $E_a \approx 19$ kJ mol^{-1}

For ZrB_2/HfB_2/SiC DLT:

$\gamma = 1.9367 \exp(-4817/T)$ up to 1800 K with $E_a \approx 40$ kJ mol^{-1}

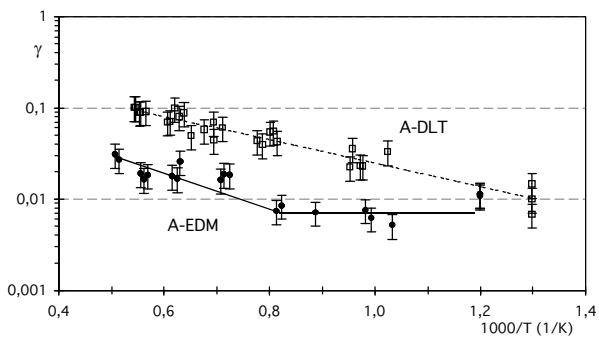

Fig. 3: Recombination coefficient for the ZrB_2/SiC (A) material with two different surface finishing – EDM and DLT– versus reciprocal temperature

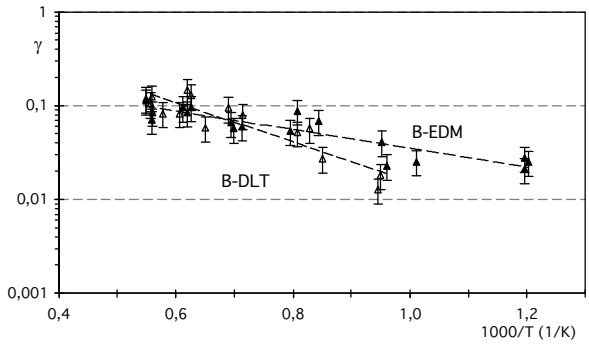

Fig. 4: Recombination coefficient for the ZrB_2/HfB_2/SiC (B) material with two different surface finishing – EDM and DLT– versus reciprocal temperature

X-ray Photoelectron Spectroscopy (XPS) was used to analyze the surfaces of the reference and tested samples after the measurement of the recombination coefficient γ. The elementary compositions have been calculated from the area of each photoelectron peak C 1s, O 1s, Si 2p, Zr 3d, B 1s and Hf 4f, using the effective ionization cross sections given by Scofield [12] and corrected by the square root of the kinetic energy of each photoelectron. The quantitative results were obtained on the surfaces after Ar^+ ion etching during 15 min under 1 kV. This treatment allows to partially remove the atmospheric carbon contamination and to carry out analysis on the atomic layers located at around 30 nm under the first contaminated layer. It has to be noticed that the carbon contamination is not totally removed. This incomplete decontamination can be due to the surface roughness (the arithmetic roughness R_a is equal to 0.58 μm for A-EDM and 0.98 for B-EDM; for A and B-DLT samples, it is lower and equal to 0.14 μm) and/or to the lower efficiency of the ion etching on insulating materials.

Table 1: Elementary composition (%) on reference and tested samples determined by XPS analysis

Compo. %	C 1s	O 1s	Si 2p	Zr 3d	B 1s	Hf 4f
A-EDM ref	21.4	53.2	9.0	12.9	3.5	-
G (1820 K)	2.6	65.2	26.8	3.4	2.0	-
K (2000 K)	13.2	59.2	2.3	25.3	-	-
A-DLT ref	30.4	35.4	6.5	12.9	14.8	-
P2 (1800 K)	3.4	61.3	31.0	0.9	3.4	-
B-EDM ref	38.6	41.9	3.5	10.6	4.7	0.7
S (1820 K)	31.6	41.9	16.5	3.8	6.2	-
B-DLT ref	23.0	38.4	5.4	15.9	15.8	1.5
W (1800 K)	1.7	64.3	28.7	2.9	2.2	0.2

Table 1 presents the elementary composition of the UHTC samples before and after treatment at high temperature under air plasma. For the ZrB_2/SiC EDM reference sample (A-EDM ref), the elementary composition close to the surface shows that it contains mainly ZrB_2 and SiC and few oxides SiO_2 and ZrO_2. After heat treatment at 1820 K (sample G), the surface is mainly composed of SiO_2 and few ZrO_2 and B_2O_3 (borosilicate glass). When the temperature is increased to 2000 K (sample K), silica vaporizes and finally the surface is mainly composed of ZrO_2. This is confirmed by the morphology of the SEM images of Fig. 5.

In Fig. 5, the micrographs of the samples A-EDM before and after high temperature and air plasma exposure are reported. The A-EDM image in Fig. 5 shows different surface morphology according to the maximum temperature used for the γ measurement. The sample after 1820 K presents a surface with a borosilicate glassy layer composed mainly of silica with small part of boron and zirconium oxides (2-3% at. detected by XPS) present as crystalline islands on the SEM image. After the γ measurement at 2000 K, the surface of the sample is mainly constituted by zirconia (crystalline as revealed by XRD) with only few traces of silica (2% at. as detected by XPS). This is due to the fact that this sample was exposed at a maximum temperature of 2000 K at which silica disappeared. Although the mechanism was not studied, the silica loss could be due to its decomposition into volatile SiO.

In Fig. 6, B-EDM and B-DLT exposed in air plasma at a maximal temperature of 1800 K show the formation of a uniform glassy layer that was confirmed to be a borosilicate glass. XPS analyses have indeed shown that the composition of the layer was mainly silica with small amounts of boron oxide (2-6 at.%), zirconia (3-4 at.%) and very small amounts of hafnia (0.2 at.%).

Even if this is not evident from the SEM micrographs, we can suppose that the different catalytic behavior of the A-EDM is related to the nature of the surface modification induced by the electrical discharge machining on this material only. Probably, the higher refractoriness of the HfB_2 included in material B limits the surface alterations occurring during EDM.

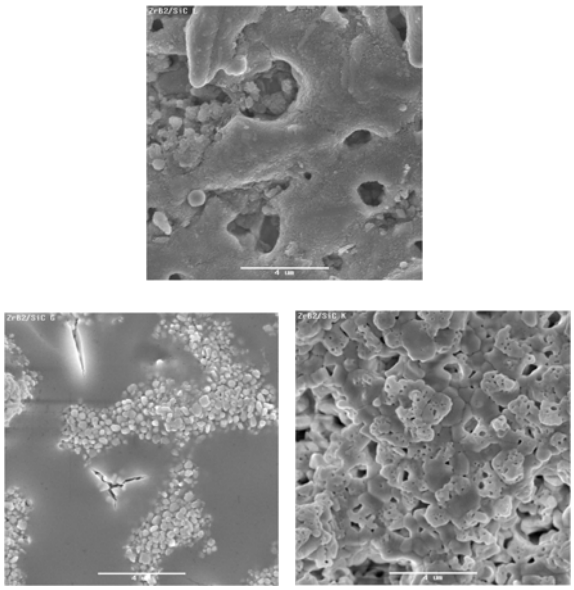

Fig. 5: SEM images of the A-EDM reference sample (top), and the two samples after γ measurement: left down, 1820 K and right down, 2000 K. The length of the scale bar is 4 μm.

With regards to catalycity measurements, the obtained results show for all the tested UHTC samples a low catalytic activity in the examined temperature range with a maximum measured value for atomic oxygen recombination coefficient γ of about 0.1 for the ZrB_2/HfB_2-based material.

DLT ZrB_2/SiC, and both EDM and DLT ZrB_2/HfB_2/SiC follow an Arrhenius type law in the whole temperature range, and they also show similar gamma values ranging from 10^{-2} about at 800 K to 10^{-1} at 1800 K. The catalytic behavior appears to be dictated again by the oxide scale that develops on the samples exposed in high temperature air plasma, regardless of the samples composition and surface finish.

On the contrary, the EDM ZrB_2/SiC sample is characterized by a peculiar catalytic behavior: in fact, at about 1200 K the kinetic equation related to the atomic oxygen recombination mechanism on the surface of EDM ZrB_2/SiC changes: for higher temperatures, the sample follows an Arrhenius type law while for lower temperatures γ becomes almost constant. This sample exhibits a minimum value of γ of about 8.10^{-3} for temperatures up to 1200 K and a maximum value of 3.10^{-2} at 2000 K. This result can be linked to the behavior observed for the γ evolution versus reciprocal temperature of the stabilized zirconia

(YSZ and CSZ) due to the presence of the monoclinic phase presented in the following section.

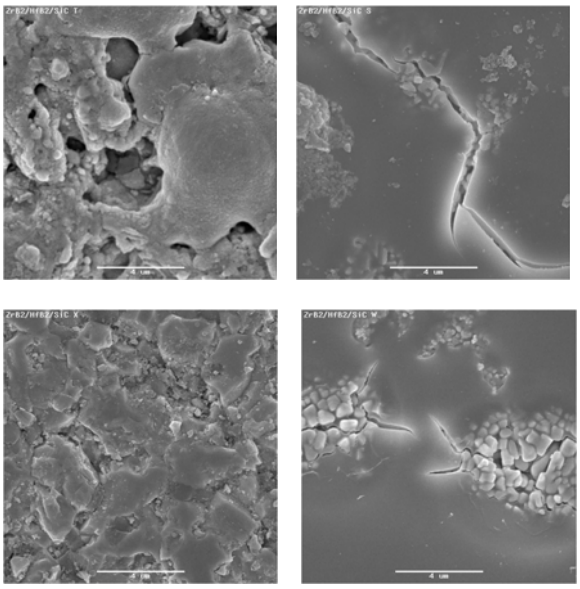

Fig. 6: SEM images of the B-EDM reference sample (left top) and after γ measurement at 1820 K (right top), and of B-DLT reference sample (left down) and after γ measurement at 1800 K (right down). The length of the scale bar is 4 μm.

4. STABILIZED-ZIRCONIA MATERIALS

The experimental results of the recombination coefficient γ versus the reciprocal temperature are obtained for the two zirconia YSZ and CSZ in the temperature range 900-2500 K, for 200 Pa total air pressure, and presented in Figs. 7 (YSZ) and 8 (CSZ).
We have to notice that, for both the zirconia stabilized with yttria (YSZ) or CaO (CSZ) around 1600 K, there is a change in the slope of the curves, due to the irreversible phase transformation from monoclinic (pattern file 83-0944) to tetragonal (pattern file 80-0965), as confirmed by the XRD pattern present in Fig. 7 for YSZ.
After catalycity measurement at the higher temperature level, the monoclinic zirconia is transformed into the tetragonal phase (and this is an irreversible process due to the sintering additives) as the temperature reached during the measurement is higher than the temperature of the sintering elaboration process. In that case when zirconia is mainly in the tetragonal phase, the recombination coefficient can be correlated by a unique Arrhenius fit (dotted lines in Figs. 7 and 8).

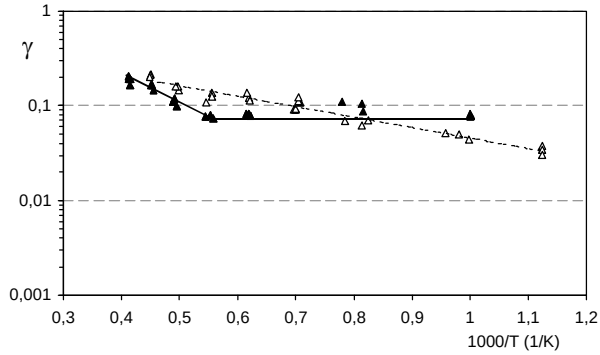

Fig. 7: Recombination coefficient for the yttria-stabilized zirconia (YSZ) versus reciprocal temperature (black triangles: 1st measurement, open triangles: 2nd one after the high temperature exposure)

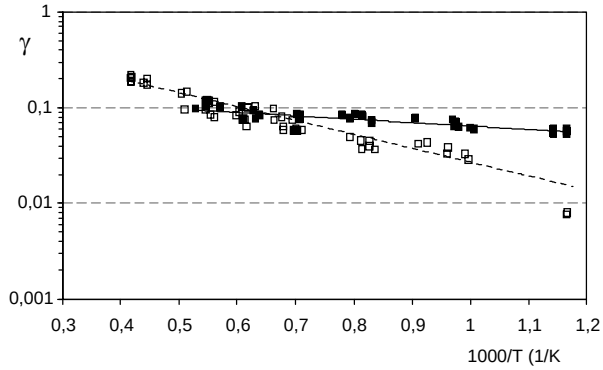

Fig. 8: Recombination coefficient for the CaO-stabilized zirconia (CSZ) versus reciprocal temperature (black squares: 1st measurement, open squares: 2nd one after the high temperature exposure)

We obtain the following expressions for the recombination coefficient γ and the respective activation energies E_a:

For the zirconia stabilized with Y_2O_3 (YSZ):
$\gamma \approx 8.10^{-2}$ until 1600 K (before the M->T phase transformation) then, $\gamma = 1.315 \exp(-4796/T)$ with $E_a \approx 40$ kJ mol^{-1} above 1600 K.
When zirconia is mainly in the tetragonal phase, then in the temperature range 900-2300 K, $\gamma = 0.579 \exp(-2544/T)$ with $E_a \approx 21$ kJ mol^{-1}

For the zirconia stabilized with CaO (CSZ):
$\gamma = 0.148 \exp(-804/T)$ and $E_a \approx 7$ kJ mol^{-1} before the M->T phase transformation.
When zirconia is mainly in the tetragonal phase, then in the temperature range 900-2500 K, $\gamma = 0.768 \exp(-3347/T)$ and $E_a \approx 28$ kJ mol^{-1}.

We can conclude that when still a fraction of monoclinic phase exists in the zirconia samples (from

about 900 to 1600 K), the evolution of the recombination coefficient is very few dependent on temperature (constant – 8.10^{-2} – taking into account the accuracy on γ) or with a very low activation energy of 7 kJ mol^{-1} but when zirconia is stabilized in the tetragonal phase (above 1600 K), the evolution of γ is more important with temperature, with mean value of E_a around 25 kJ mol^{-1}. The data obtained for YSZ and CSZ after 1600 K are nearly the same. The γ coefficient increases with temperature from 0.04 at 1000 K up a maximum value of 0.20 for 2400 K for both YSZ and CSZ zirconia ceramics, when the tetragonal phase is mainly present.

Fig. 9 presents the XRD patterns of the sample YSZ before and after the measurement of γ at high temperature. In this figure, the monoclinic (M) phase has nearly disappeared for the YSZ material after high temperature exposure, in agreement with the results obtained for the recombination coefficient. These results confirm the influence of the crystalline structure of the material upon its catalycity as we have already proved on silica polymorphs [9].

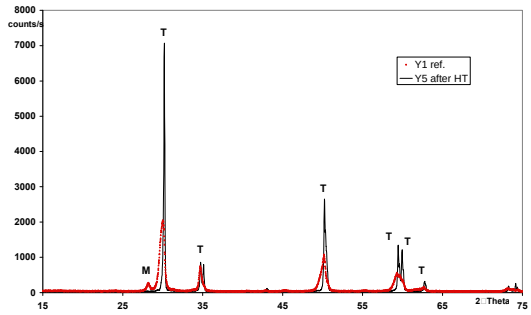

Fig. 9: XRD pattern of the YSZ zirconia before (in red) and after (in black) the higher temperature measurement

5. COMPARISON OF THE CATALYCITY OF SEVERAL OXIDES

Since several years, we have measured the recombination of atomic oxygen on some surfaces submitted to high temperature and air plasma exposure [9, 10]. Fig. 10 reports in a reduced temperature range – 1100-2400 K – the data obtained for silica formed during the oxidation of sintered SiC – β-cristobalite –, silica in form of quartz, alumina on sintered AlN and for the sintered yttria-stabilized zirconia YSZ and the ZrB_2/SiC EDM (material A) detailed in this paper.

For this temperature range, sintered zirconia, β-cristobalite and alumina on AlN present recombination coefficients very close, the higher values being obtained for alumina.

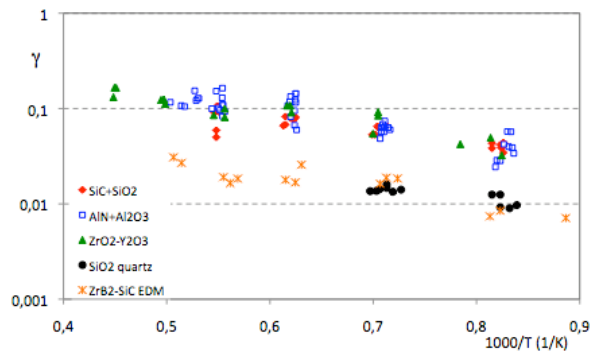

Fig. 10: Evolution of the recombination coefficient versus reciprocal temperature for several oxide ceramics.

On the contrary, ZrB_2/SiC EDM and quartz have lower values of γ on the same temperature range, this being due to the fact that the borosilicate glass containing zirconia and formed during oxidation of the UHTC material has the same behavior than the quartz glass, the glass structure being favorable to lower the recombination of atoms. In that case, for temperature up to 2000 K, zirconium-based UHTC are better as protective materials for atmospheric re-entry than aluminum and silicon-based materials.

6. CONCLUSIONS

The experimental determination of the recombination coefficient on stabilized zirconia and on UHTC materials of different composition and surface mechanical treatment has been realized in the MESOX set-up.

Zirconia samples were used to show the influence of sintering aids, but finally, the main influence observed is the one due to the irreversible phase transformation from monoclinic to tetragonal. Sintered zirconia samples present recombination coefficient ranging from 8.10^{-2} at 900 K to 0.2 at 2400 K after stabilization of the tetragonal phase.

The use of UHTC to manufacture thermal protection systems (TPS) and increase the heat resistance for sharp-shaped hypersonic re-entry vehicles needs the complete characterization of their radiative and catalytic properties. The recombination coefficient of atomic oxygen for sintered zirconium diboride-based composite ceramics – ZrB_2/SiC and ZrB_2/HfB_2/SiC – was measured as a function of temperature. Moreover, in order to describe the effect of the machining method on catalycity, two kinds of surface manufacturing were

considered: samples manufactured by electrical discharge machining (EDM) and machined by diamond-loaded tools (DLT). Finally, these samples present a low catalytic activity when a borosilicate glassy layer with small parts of zirconia is formed on the surface – below 1800 K – and when zirconia is present in higher quantity, then the recombination coefficient can be close to 0.1 at 2000 K. Moreover, the presence of HfB_2 in material B led to higher recombination coefficients, probably due to the higher catalycity of hafnia compared to zirconia.

In-depth microstructural investigation by SEM and XPS analyses performed in this study has shown that the evolution of the recombination coefficient with temperature in atmospheric re-entry conditions is sensitive to surface composition and morphology in UHTC ceramics. This study highlighted the extreme complexity of UHTC oxidation behavior, as well as the need of an exhaustive knowledge of the phenomena regulating surface oxidation in order to explain the surface properties of this class of materials.

Future prospects are to extend the method developed for the measurement of the recombination coefficient to CO_2 plasma for new missions with martian entry, without any assumption on the equality between γ_O and γ_{CO}. Preliminary works on CO_2 plasma have been performed for the determination of the thermal flux of recombination transferred to the material and the measured thermal flux was nearly twice the value obtained under air plasma conditions on silicon carbide based materials.

7. REFERENCES

1. Kolodziej P., Salute J., Keese D.L., First flight demonstration of a sharp Ultra High-Temperature Ceramic nosetip, *NASA TM-112215*, Dec. 1997.
2. Chamberlain A., Fahrenoltz W.G., Hilmas G.E., Ellerby D., Oxidation of ZrB_2-SiC ceramics under atmospheric and reentry conditions, *Refr. Appl. Trans.*, 1, 1-8, 2005.
3. Monteverde F., Bellosi A., Scatteia L., Processing and properties of Ultra High Temperature Ceramics for space applications, *Mater. Sci. Engineering A*, 485, 415-421, 2008.
4. Monteverde F., Bellosi A., Guicciardi S., Processing and properties of zirconium diboride-based composites, *J. Eur. Ceram. Soc.*, 22, 279-288, 2002.
5. Fahrenholtz W.G., Hilmas G.E., Talmy I.G., Zaykoski J.A., Refractory diborides of zirconium and hafnium, *J. Am. Ceram. Soc.*, 90, 1347-1364, 2007.
6. Marschall J., Chamberlain A., Crunkleton D., Rogers B., Catalytic atom recombination on ZrB_2/SiC and HfB_2/SiC Ultra High-Temperature Ceramic composites, *J. Spacecraft & Rockets* 41 (4), 576-581, 2004.
7. Scatteia L., Borrelli R., Cosentino G., Bêche E., Sans J.L., Balat-Pichelin M., Catalytic and radiative behaviors of ZrB_2-SiC Ultra High-Temperature Ceramic Composites, *J. Spacecraft & Rockets*, 43 (5), 1004-1012, 2006.
8. Scatteia L., Alfano D., Monteverde F., Sans J.L., Balat-Pichelin M., Effect of the machining method on the catalycity and emissivity of ZrB_2 and ZrB_2-HfB_2-based ceramics, *J. Am. Ceram. Soc.*, 91 (5), 1461-1468, 2008.
9. Balat-Pichelin M., Badie J.M., Berjoan R., Boubert P., Recombination coefficient of atomic oxygen on ceramic materials under Earth re-entry conditions by Optical Emission Spectroscopy, *Chem. Phys.* 291 (2), 181-194, 2003.
10. Balat-Pichelin M., Bedra L., Gerasimova O., Boubert P., Recombination of atomic oxygen on alpha-Al_2O_3 at high temperature under air microwave-induced plasma, *Chem. Phys.* 340 (1-3), 217-226, 2007.
11. Balat-Pichelin M., Vesel A., Neutral oxygen atom density in the MESOX air plasma solar furnace facility, *Chem. Phys.*, 327 (1), 112-118, 2006.
12. Scofield J.H., Hartree-Slater subshell photo-ionization cross-sections at 1254 and 1487 eV, *J. Electr. Spectrosc. & Related Phenom.* 8, 129-137, 1976.